



Preyssler type heteropolyacid-incorporated highly water-selective sodium alginate-based inorganic–organic hybrid membranes for pervaporation dehydration of ethanol

Veeresh T. Magalad, Amit R. Supale, Sanjeev P. Maradur, Gavisiddappa S. Gokavi*, Tejrav M. Aminabhavi¹

Department of Chemistry, Shivaji University, Vidyanagar, Kolhapur, 416 004, Maharashtra, India

ARTICLE INFO

Article history:

Received 15 September 2009

Received in revised form 15 February 2010

Accepted 20 February 2010

Keywords:

Pervaporation

Preyssler type heteropoly acid

Sodium alginate

Ethanol–water mixture

Separation factor

ABSTRACT

Sodium alginate (NaAlg) hybrid membranes containing 6, 8 and 10 wt.% of Preyssler type heteropolyacid $H_{14}[NaP_5W_{30}O_{110}]$ (HPA) were prepared and characterized by FTIR, SEM, TGA, DSC, UTM and contact angle measurements. Hybrid membranes were more hydrophilic than pristine NaAlg membrane and exhibited increased pervaporation separation index (PSI) for selectively separating water from the azeotropic mixture (4 wt.% water + 96 wt.% ethanol) with ethanol. The highest separation factor of 59,976 with a flux of $0.043 \text{ kg/m}^2 \text{ h}$ was obtained for the hybrid membrane i.e., NaAlg-6, which was further investigated in greater details to study the effect of feed water composition on its pervaporation (PV) performance. All the membranes were mechanically stable as tested by UTM during the PV operations. Degree of swelling and sorption selectivity values increased with increasing feed water composition giving a decrease in separation factor. Flory–Huggins-type interaction parameter for water and ethanol were computed to offer thermodynamic explanations. Membranes of this study are highly water-selective. Activation energies for total permeation, permeation of water and ethanol were determined at various temperatures. The negative heat of sorption indicates the predominance of Langmuir sorption mode for NaAlg-6 hybrid membrane.

© 2010 Elsevier B.V. All rights reserved.

1. Introduction

Aqueous ethanol solutions are produced during the fermentation of disposed biomass. Ethanol is used as a renewable source of energy to replace conventional petroleum products. Purification and concentration of aqueous ethanol mixtures are carried out by distillation, but at the azeotropic composition, it becomes difficult to separate the mixture by conventional distillation, without recourse to benzene, a carcinogen. Alternatively, novel polymeric membranes have been developed and used to separate/concentrate aqueous ethanol solutions using pervaporation (PV) technique [1–4]. The main focus in these studies is to achieve high separation factor and flux for one of the components of the mixture for an efficient separation. Natural polymer such as sodium alginate (NaAlg) has been widely used previously in PV separation due to its hydrophilic nature and good flexibility [2–9]. However, swelling of NaAlg membrane in aqueous media limits its application. In order to overcome these difficulties, attempts have been made to mod-

ify to improve the stability of NaAlg membranes required in PV operation.

In the prior art, Yeom and Lee [10] have developed glutaraldehyde-crosslinked NaAlg membrane and used it for the PV separation of water–isopropanol mixture. It was found that as the crosslinking increases, separation factor to water also increases, while flux decreases. Moon et al. [11] have prepared novel two-ply dense composite membranes of NaAlg and chitosan for dehydration of isopropanol and ethanol. They reported that two-ply membranes showed better PV performance and mechanical strength properties than the pristine NaAlg membrane. Many attempts have been made to increase the membrane performance of NaAlg by modifications such as blending [12], grafting [13,14], crosslinking [15], or by adding filler particles [16–19].

Recently, much work has been done using different kinds of HPAs [20–24] such as phosphotungstic acid hydrate (HPW), silicotungstic acid hydrate (HSiW) and phosphomolybdic acid (HPMo) in developing proton conducting membranes. Due to their strong acidic, catalytic and hydrophilic properties, these can be used as fillers to enhance the membrane barrier properties. Heteropolyacids are known for their discrete structures containing a large anion and mobile protons in the form of H^+ , H_3O^+ , $H_5O_2^+$, etc. [25]. Preyssler anion has an excellent hydrolytic stability between pH 1

* Corresponding author. Tel.: +91 231 2609167; fax: +91 231 2692333.

E-mail address: gsgokavi@hotmail.com (G.S. Gokavi).

¹ CSIR Emeritus Scientist, New Delhi, India.

Nomenclature

M_s and M_d	weights of swollen and dry membranes
A	effective membrane area (m^2)
J	flux ($kg/m^2 h$)
J_0	pre-exponential factor for permeation
t	permeation time (h)
W_i	weight of permeate (kg)
P and F	weight percent of permeate and feed
PSI	pervaporation separation index
R	gas constant
T	temperature in Kelvin
ΔH_s	heat of sorption (kJ/mol)

Greek letter

β_{ij}	separation factor
α_s	sorption selectivity
α_d	diffusion selectivity
χ_{ip}	Flory–Huggins interaction parameters between solvent and polymer
δ	solubility parameter

and 12 and demonstrates its functionality over a wide range of pH. The incorporation of such HPAs in the polymer matrix facilitates its interaction with the solvent molecules, especially with water due to the presence of hydrated protons.

To the best of our knowledge, no reports are yet available on the use of Preyssler type HPA-filled NaAlg membranes used in PV dehydration of ethanol. The present study is aimed at preparing Preyssler type HPA-filled NaAlg hybrid composite membranes by incorporating different amounts of HPA (6, 8 and 10 wt.% with respect to wt.% of NaAlg) into NaAlg matrix to improve the membrane performance to water. Further, FTIR, SEM, TGA and DSC characterizations were done to understand chemical interactions of filler particles with the base NaAlg matrix, membrane morphology and thermal properties, respectively. Membranes were sturdy as tested by UTM. Effects of HPA content on PV separation, degree of swelling and sorption properties, feed water composition and feed temperature on the PV performance of membranes are investigated.

2. Experimental

2.1. Materials

Sodium alginate, orthophosphoric acid, sodium tungstate, and potassium chloride were all purchased from s.d. Fine Chemicals, Mumbai, India. All the chemicals were of reagent grade and used without further purification. Double distilled water was used throughout the study.

2.2. Preparation of Preyssler type heteropolyacid

Orthophosphoric acid (75 cm³, 90%, 1.2 mol) was slowly added to a solution containing 99 g of sodium tungstate (0.3 mol) in 50 cm³ water at 45 °C. The resulting mixture was refluxed for 5 h, cooled to ambient temperature (30 °C) and diluted with 15 cm³ of water. Powdered potassium chloride (22.5 g, 0.32 mol) was slowly added to the vigorously stirred solution for about 35 min at ambient temperature. The pale green impure precipitate was filtered and washed off with 0.1 M potassium acetate. The white needle like crystals of potassium salt of Preyssler anion was recrystallized from hot water. The free acid was prepared by passing a solution of potassium salt of Preyssler anion in 20 cm³ water through a col-

umn (50 cm × 1 cm) of Dowex-50WX in H⁺ form. Evaporation of elute to dryness under vacuum afforded the desired HPA viz., H₁₄ [NaP₅W₃₀O₁₁₀] [26].

2.3. Membrane preparation

NaAlg (4 g) was dissolved in 100 mL of water with constant stirring. To this solution 6, 8 and 10 wt.% of Preyssler HPA in water were added and stirred for 24 h. The homogeneous solution was then cast uniformly onto a glass plate with the help of a doctor's knife and dried at ambient temperature (30 °C). The thickness of the membranes measured by micrometer screw gauge was around 40 μm ± 2 μm. The membranes containing 6, 8 and 10 wt.% Preyssler HPA into NaAlg are designated, respectively as NaAlg-6, NaAlg-8, and NaAlg-10. The pristine NaAlg membrane was prepared in the same manner in the absence of Preyssler HPA and designated as NaAlg-0.

2.4. Membrane characterization

FTIR spectra of Preyssler HPA, pure NaAlg as well as HPA-loaded NaAlg membranes were scanned from 400 to 4000 cm⁻¹ using Nicolet, Impact-410, USA, FTIR spectrophotometer by the KBr pellet method. Surface morphology of NaAlg-6, NaAlg-8 and NaAlg-10 membranes were obtained at 10 kV with a JSM-840A scanning electron microscope (JEOL, Tokyo, Japan). Since these films were non-conductive, gold coating of 10 nm thickness was done on the samples. DSC and TGA thermograms of NaAlg-0 and NaAlg-6 were obtained using SDT 2960 simultaneous DSC-TGA (TA Instruments, USA). Measurements were performed over the temperature range of 25–600 °C at the heating rate of 10 °C/min. The sample pan was conditioned in the instrument before performing the experiment. Static contact angles between water and the membranes were measured using a contact angle meter (Ramehart, Model 500-F1, USA) at 30 °C. Tensile strength and Young's modulus of NaAlg-0, NaAlg-6, NaAlg-8 and NaAlg-12 membranes were measured using the universal testing machine (UTM Model H25 KS, Hounsfield, Surrey, United Kingdom). Test specimens were prepared in the form of dumbbell shapes as per ASTM D-638 standards. Films of gauge length of 50 mm and width of 10 mm were stretched at the crosshead speed of 10 mm/min.

2.5. Degree of swelling and sorption experiments

Swelling experiments were performed gravimetrically at 30 °C on the membranes in 10, 20, 30 and 40 wt.% water containing feed mixtures. Initial mass of the circularly cut ($d_{ia} = 3$ cm) membrane was taken by placing them on a single-pan digital microbalance (model AE 240, Mettler, Switzerland) sensitive to ±0.01 mg. Samples were then placed inside the specially designed airtight test bottles containing 30 cm³ of the test solvent and the bottles were transferred to a hot-air oven maintained at 30 °C for 48 h. Mass of the swollen membranes was measured immediately by removing the test samples from the bottles and wiping the surface-adhered liquid droplets by gently pressing between filter paper wraps. The sorbed liquids were recovered in a liquid nitrogen trap by desorbing equilibrated sample in the purge and trap apparatus and analyzed by gas chromatography. The % degree of swelling, DS was calculated as:

$$DS(\%) = \left(\frac{M_s - M_d}{M_d} \right) \times 100 \quad (1)$$

where M_s and M_d are weights of the swollen and dry membranes, respectively.

The solubility selectivity, α_s was calculated as:

$$\alpha_s = \left(\frac{M_w}{M_e} \right) \times \left(\frac{F_e}{F_w} \right) \quad (2)$$

where M_w and M_e are the mass fractions of water and ethanol in the membrane, and F_w and F_e are those of water and ethanol in the feed, respectively.

According to solution-diffusion mechanism, the diffusion selectivity, α_d was calculated as follows:

$$\alpha_d = \frac{\beta_{ij}}{\alpha_s} \quad (3)$$

where β_{ij} is a separation factor. Considering the volatile characteristics of ethanol, all the sorption experiments were done at least three times and the experimental errors were maintained within $\pm 3\%$.

2.6. Pervaporation experiment

Pervaporation experiments were performed in an apparatus that was indigenously designed; detailed protocols have been described elsewhere [27]. Effective area of the membrane in the PV cell was 26.43 cm^2 with a liquid volume capacity of 200 cm^3 . PV apparatus consists of a stainless steel cell in which feed stock solution was maintained at the required temperature by a thermostatically controlled water jacket. PV cell consists of an efficient three-blade stirrer powered by a DC motor in the feed compartment. The feed mixture was stirred at 200 rpm, the downstream pressure was maintained at 5 mbar using a vacuum pump (Model: ED-21, Hindhivac, Bangalore, India).

Before starting the PV experiment, test membrane was equilibrated for 3 h with feed mixture and after establishment of the steady state; liquid permeate was collected and condensed in traps using liquid nitrogen. Permeate sample was collected for up to 8–10 h. The collected permeate was weighed after allowing it to attain room temperature using a digital microbalance sensitive to $\pm 0.01 \text{ mg}$ to determine the flux, which was then analyzed by gas chromatography (Model: Ultima-2100, Netel India, Ltd, Mumbai) to calculate separation factor as explained below.

2.6.1. Flux and separation factor

In PV, flux, J of the fast permeating component, i from the binary liquid mixture comprising i (water) and j (ethanol) is calculated as:

$$J_i = \frac{W_i}{A \times t} \quad (\text{kg/m}^2 \text{ h}) \quad (4)$$

where W_i is weight of the permeate (kg), A is effective area of the membrane (m^2) and t is permeation time (h). Separation factor was calculated from the respective concentrations of components in the feed and permeate using:

$$\beta_{ij} = \left(\frac{P_w}{P_e} \right) \times \left(\frac{F_e}{F_w} \right) \quad (5)$$

where P_w and P_e are wt.% of water and ethanol in permeate, F_w and F_e are wt.% of water and ethanol in feed, respectively. The compositions of feed and permeate were measured by gas chromatography (Model: Ultima-2100, Netel India Pvt Ltd, Mumbai) using thermal conductivity detector (TCD) and Porapak Q column of 2 m length by maintaining the oven temperature at 70°C (isothermal), while injector and detector temperatures were maintained at 150°C . The sample injection size was $1 \mu\text{L}$ and ultra pure hydrogen was used as a carrier gas at a pressure of 1 kg/cm^2 . The GC response was calibrated for this particular column and conditions with known compositions of water–ethanol mixtures and calibration factors were fed into the software to obtain the correct analysis for unknown sample [15].

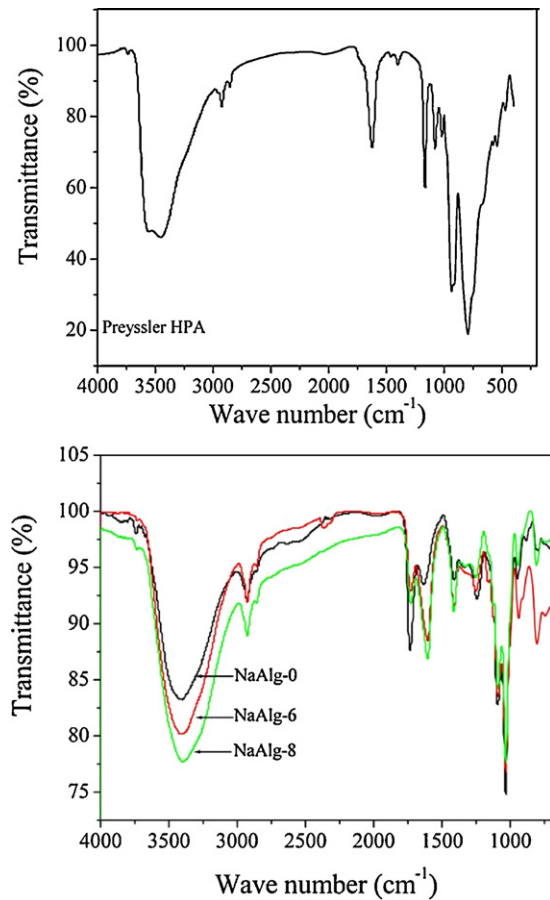


Fig. 1. FTIR spectra of Preyssler HPA, NaAlg-0, NaAlg-6 and NaAlg-8.

Pervaporation separation index (PSI) measures the separation capability of the membrane, which was calculated as [28]:

$$\text{PSI} = J \times \beta \quad (6)$$

It may be noted that after continuously using the PV membranes for more than 8 h, membranes were quite sturdy without showing any degradation.

3. Results and discussion

3.1. Membrane characterization

3.1.1. FTIR studies

FTIR spectra of Preyssler HPA, NaAlg-0, NaAlg-6 and NaAlg-8 membranes are presented in Fig. 1. HPA shows all FTIR vibration peaks assigned to a Preyssler structure [29]. The P–O stretching vibrations are observed at 1163, 1079 and 1023 cm^{-1} with P–O bending at 573 cm^{-1} . The stretching frequencies of W–O–W and W=O are observed at 940 and 787 cm^{-1} , respectively. The spectrum of NaAlg-0 shows prominent peaks of C=O stretching of the carboxylic group at 1651 cm^{-1} , C–H group at 2943 cm^{-1} , while its characteristic free –OH is observed around $3188\text{--}3583 \text{ cm}^{-1}$. There is a slightly red-shift of –OH absorption from 3411 cm^{-1} of NaAlg-0 to 3395 cm^{-1} for NaAlg-6 and 3384 cm^{-1} for NaAlg-8 membranes. Comparing the FTIR spectra of Preyssler HPA with NaAlg-6 and NaAlg-8 hybrid membranes, we find that no characteristic bands of Preyssler structure units are found in FTIR spectrum of the hybrid membranes, suggesting a good distribution of Preyssler HPA particles in NaAlg matrix [30]. The –OH absorption bands are stronger for NaAlg-8 (at 3384 cm^{-1}) and NaAlg-6 (at 3395 cm^{-1}) than for

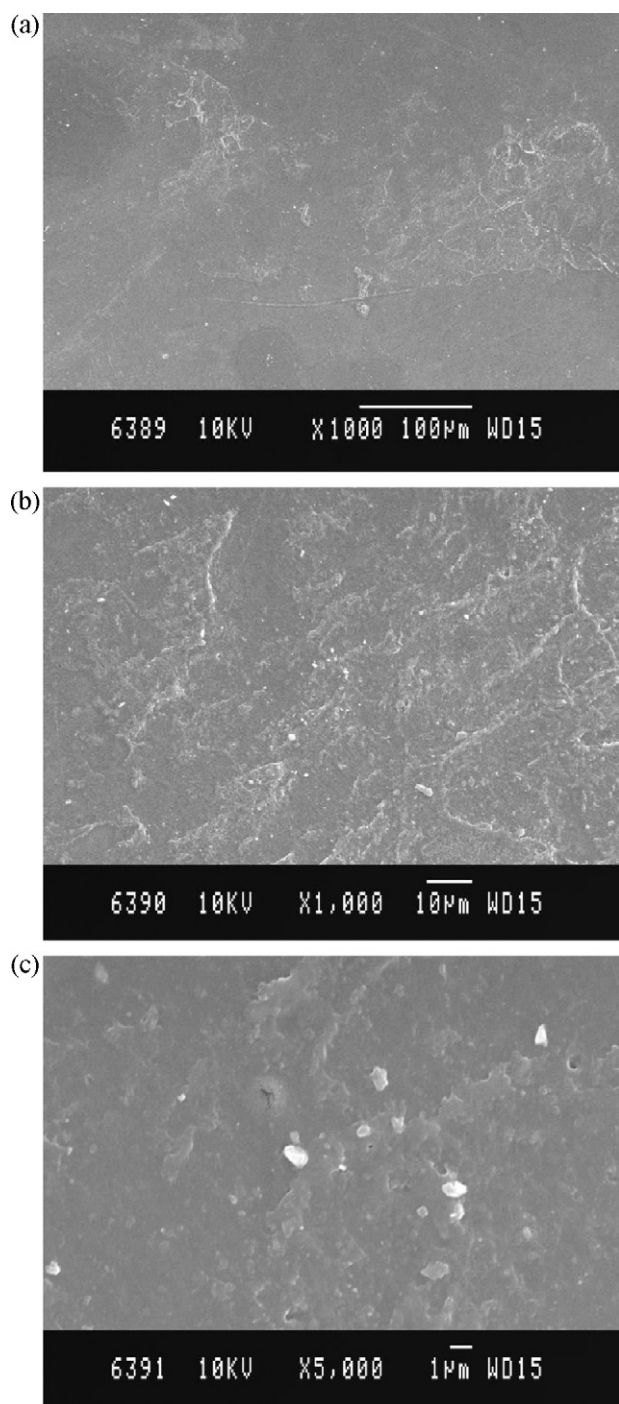


Fig. 2. Surface scanning electron micrographs of (a) NaAlg-6, (b) NaAlg-8 and (c) NaAlg-10 membranes.

NaAlg-0 membrane (at 3411 cm^{-1}), suggesting that the developed hybrid membranes possess higher hydrophilicity than plain NaAlg membrane.

3.1.2. Scanning electron microscopy

SEM of HPA-filled NaAlg membranes was performed to study the distribution of HPA filler particles in the membranes. SEM images shown in Fig. 2(a)–(c) reveal that NaAlg-6 membrane shows distribution of HPA particles, which is more evident at higher loadings. This type of morphology in the membrane would facilitate high water transport through the membrane due to the restricted transport of somewhat less polar ethanol.

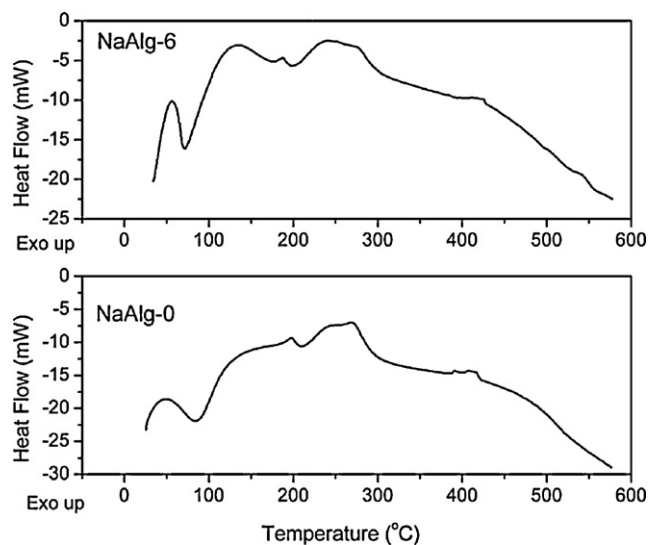


Fig. 3. DSC thermograms of NaAlg-0 and NaAlg-6 membranes.

3.1.3. DSC analysis

DSC curves of NaAlg-0 and NaAlg-6 are shown in Fig. 3. In the case of NaAlg-0, a sharp endothermic melting curve in the range of $190\text{--}203^\circ\text{C}$ i.e., at 197.7°C represents the melting point, but the melting endotherm range has shifted to $175\text{--}195^\circ\text{C}$ in case of NaAlg-6, which may be ascribed to its reduced crystallinity due to the incorporation of HPA into the NaAlg matrix. However, the order of melting range for these membranes is: NaAlg-0 ($203^\circ\text{C} - 190^\circ\text{C} = 13^\circ\text{C}$) > NaAlg-6 ($195^\circ\text{C} - 175^\circ\text{C} = 20^\circ\text{C}$), which confirms the decrease in the extent of crystallization of NaAlg-6 from NaAlg-0 [31]. Therefore, the incorporation of an inorganic filler, such as HPA into NaAlg matrix is evidenced by the order of melting range, in both the membranes analyzed.

3.1.4. TGA analysis

TGA thermograms of NaAlg-0 and NaAlg-6 membranes shown in Fig. 4 exhibit two major weight loss regions with an onset of maximum weight loss at its melting temperature at 200°C , which continues up to 350°C . The weight losses of these membranes in different temperature regions are associated with the splitting of the main chain and final decomposition of the polymer. It is observed that the extent of weight loss during melting

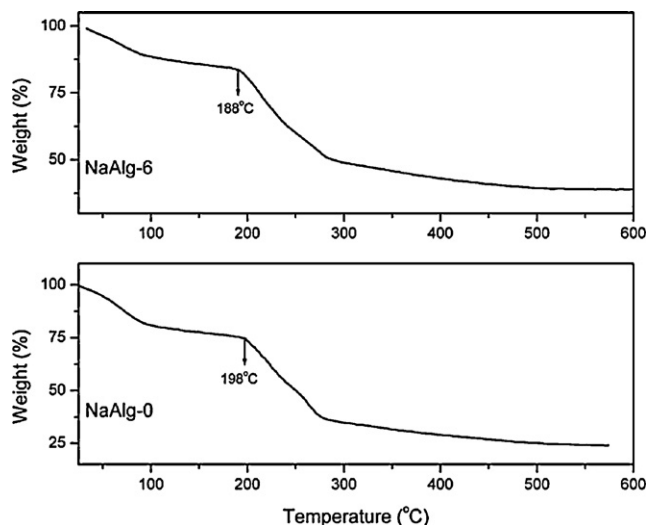


Fig. 4. TGA curves of NaAlg-0 and NaAlg-6 membranes.

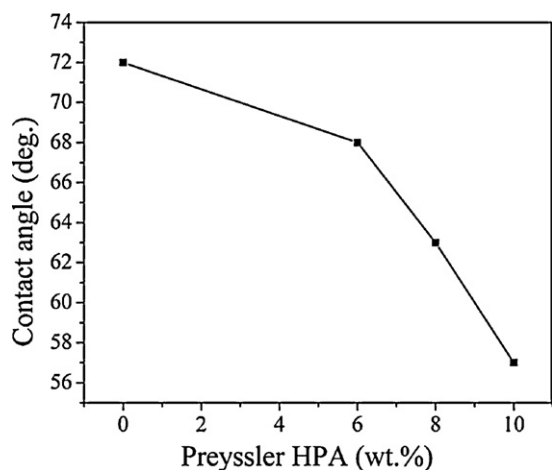


Fig. 5. Effect of HPA content on contact angle between water and membranes.

of the polymers follows the sequence: NaAlg-0 (46.7%) > NaAlg-6 (40.4%); this trend is attributed to increasing order of thermal stability from NaAlg-0 to NaAlg-6 membrane due to HPA loading. It is also observed that wt.% residue after thermal decomposition of the matrix at 500 °C is higher for NaAlg-6 than NaAlg-0, indicating the presence of HPA filler in the NaAlg matrix, since HPA filler remains intact even at this temperature.

3.1.5. Contact angle measurement

The contact angle between water and membrane surface is used as measure of membrane hydrophilicity. Smaller the contact angle, greater will be hydrophilicity of the membrane. Fig. 5 shows that contact angles of the membranes with water continuously decrease from 72° to 57°. This type of linear decrease in contact angle from NaAlg-0 to NaAlg-10 indicates that HPA-incorporated membranes are more hydrophilic than nascent NaAlg.

3.1.6. Mechanical stability

Tensile strength and Young's modulus of all the membrane samples measured by UTM indicated adequate mechanical strengths. Hence, the present membranes are stable and safe to use in PV runs. These values varied, depending upon the filler loadings. For instance, the results of tensile strengths ($\text{N/m}^2 \times 10^{-5}$) of NaAlg-0, NaAlg-6, NaAlg-8, and NaAlg-12 are 4.4, 4.8, 5.4 and 7.2, respectively; whereas, the corresponding Young's modulus (MPa) are: 16.2, 18.7, 32.6 and 38.1, respectively; these data indicate increased mechanical strength with increasing filler loadings.

3.2. Effect of addition of HPA on PV performance

Table 1 displays the results of flux, separation factor and PSI for different membranes. Clearly the addition of the HPA into NaAlg matrix has improved the PV dehydration performance of the composite hybrid membranes at azeotropic composition of 96 wt.% of ethanol at 30 °C under 5 mbar pressures. The fluxes of NaAlg composite hybrid membranes (NaAlg-6, NaAlg-8 and NaAlg-10) increase systematically with increasing loading of HPA compared

Table 1
Effect of addition of Preyssler HPA on PV performance of NaAlg membranes at azeotropic feed composition of 4 wt.% water at 30 °C and 5 mbar pressure.

Membrane	J ($\text{kg/m}^2 \text{ h}$)	β_{ij}	PSI
NaAlg-0	0.021	55	1.2
NaAlg-6	0.043	59,976	2580
NaAlg-8	0.049	21,794	1068
NaAlg-10	0.070	6291	440

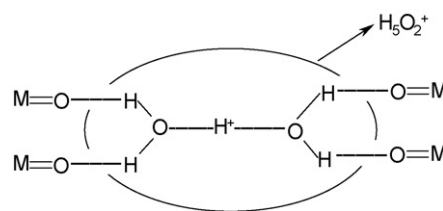


Fig. 6. Schematic structure of bulk proton sites in HPAs.

to the pristine NaAlg membrane due to hydrophilic nature of the filler that absorbs selectively more of water molecules; but there is a drastic decrease in separation factor from 59,976 to 6291 for NaAlg-6 to NaAlg-10 membrane compared to NaAlg-0 membrane, which offered a separation factor of 55. This effect is attributed to the discrete active surface sites of solid heteropolyacids, such as heteropolyanions and counter cations viz., H^+ , H_3O^+ , H_5O_2^+ , etc. [25]. These counter cations are found between the HPA units through hydrogen bonding to the terminal oxygens as shown in Fig. 6, which make them to behave like solutions and absorb good amount of water due to the formation of HPA solvates in the membranes. Thus, in the presence of excess water, increased interaction of HPA with water would result in favorable formation of hydrated protons, thereby giving a rise in separation factor for water.

Pervaporation separation index (PSI), which is the product of permeation rate and separation factor is a measure of PV separation ability of a membrane for the feed mixture. As displayed in Table 1, the NaAlg-6 membrane showed the highest PSI of 2580 compared to NaAlg-8 and NaAlg-10 membranes, whose values are systematically smaller. Therefore, NaAlg-6 membrane was used for detailed investigation. However, for NaAlg-0, the PSI value is extremely smaller viz., 1.2 compared to the hybrid membranes.

3.3. Degree of swelling and sorption

The results of % degree of swelling of NaAlg-6 membrane in water-ethanol mixture at various compositions are presented in Table 2. For NaAlg-6 membrane, the % degree of swelling is 5.2% in pure ethanol, whereas in pure water, % degree of swelling is 165%, indicating relatively higher affinity of the membrane towards water, than ethanol. The % DS increased from 43 to 77% with increasing feed water composition from 5 to 40 wt.%, also resulting in a systematic increase of water flux, with a concomitant decrease in separation factor from 47,481 to as low as 86.

Mass transfer through organic barrier membrane is assumed to follow sorption-diffusion model, which involves (i) upstream sorption of the mixture onto the surface of the membrane that induces initial partitioning of the feed that is mainly dependent on physicochemical properties of the polymer; (ii) relative diffusion of penetrant molecules through dense membranes and (iii) permeant vaporization at the downstream side of the membrane that does not influence much on the transport process as long as the downstream side vapor pressure of each liquid component remains below its respective saturated vapor pressure. In any membrane-

Table 2
Effect of feed water composition on degree of swelling, permeate water composition, flux and separation factor of water for NaAlg-6 membrane. (experimental conditions: membrane thickness $40 \mu\text{m} \pm 2 \mu\text{m}$ at 30 °C and 5 mbar pressure).

F_w (wt.%)	DS (%)	P_w (wt.%)	J ($\text{kg/m}^2 \text{ h}$)	β_{ij}
5	43	99.96	0.06	47,481
10	53	99.94	0.14	14,991
20	62	99.51	0.18	812
30	73	99.43	0.21	407
40	77	98.30	0.23	86

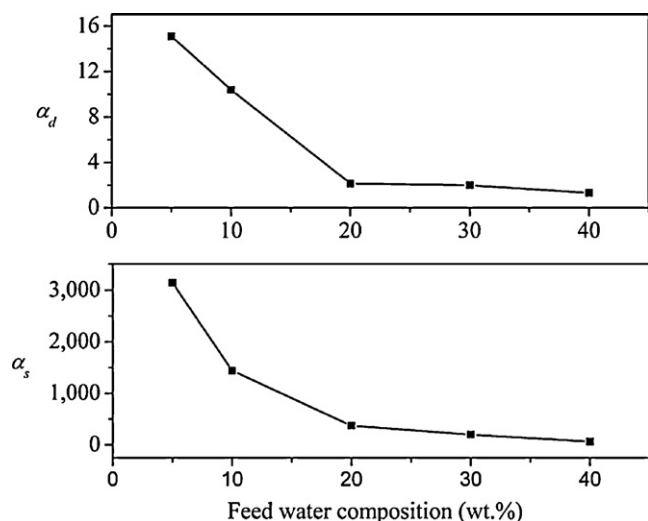


Fig. 7. Sorption selectivity (α_s) and diffusion selectivity (α_d) of NaAlg-6 membrane at different feed water compositions.

based separation process, sorption and diffusion of liquids play a dominant role, since these are closely linked to govern the membrane performance during the PV operation.

Fig. 7 shows the effect of feed water composition on sorption selectivity (α_s) and diffusion selectivity (α_d) of NaAlg-6 membrane, wherein solubility selectivity is much higher than diffusion selectivity at all feed water compositions, suggesting that diffusion plays a minor role during the PV separation. In order to investigate membrane–solvent interaction, the polymer–solvent interaction parameter, χ , was calculated using Flory–Huggins-type equation [32–34]:

$$\chi_{ip} = \frac{V_i (\delta_p - \delta_i)^2}{RT} \quad (7)$$

where δ_i is solubility parameter ($J^{1/2} \text{ cm}^{-3/2}$) of the *i*th component. Solubility parameter, δ of NaAlg polymer was estimated to be $61.48 J^{1/2} \text{ cm}^{-3/2}$ on the basis of atomic group contribution method [35]. Solubility parameters of water and ethanol solvents were taken from the literature [36]. The quantities V_i , R and T are molar volume of solvent, universal gas constant and temperature in Kelvin (K), respectively.

Fig. 8 shows the interaction parameters for NaAlg-6 membrane with different feed compositions of water. It is found that interaction parameters of water with the membrane (χ_{1p}) and ethanol with the membrane (χ_{2p}) show a decrease with increasing feed water composition. Stronger interaction between the components of the mixture and polymer results in a smaller value of interaction parameter [37]. In the present study, NaAlg-6 membrane has lower χ_{1p} values, but higher χ_{2p} values at all feed water compositions, indicating that the present membranes are water-selective.

3.4. Effect of feed water composition

PV performance of the membranes at 30 °C was investigated for NaAlg-6 membrane by varying feed water compositions from 5 to 40 wt.%, keeping the permeate pressure at 5 mbar and membrane thickness at 40 μm as constant. Resulting values of flux and separation factor data are displayed in Table 2, which suggest an increase in flux from 0.062 to 0.234 $\text{kg/m}^2 \text{ h}$, while separation factor decreased from 47,481 to 86 with increasing feed water composition from 5 to 40 wt.%. Thus, absorption of large amount of water at higher feed concentration of water might be responsible for the polymer plasticization effect in the presence of excess amount of

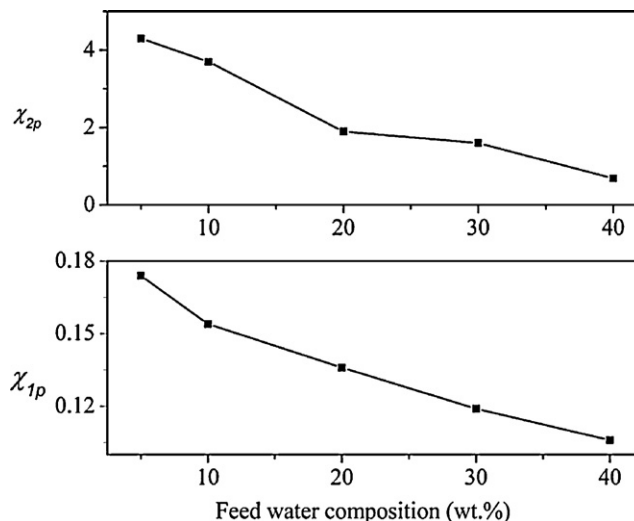


Fig. 8. Interaction parameters for NaAlg-6 membrane at different feed water compositions.

water, resulting in an increase of flux with the decrease in separation factor.

In the case of hybrid composite NaAlg-6 membrane, the selective separation of water from ethanol is due to the combined effect of hydrophilic–hydrophilic interactions between Preyessler HPA and NaAlg with water molecules in addition to the effect of polymer plasticization as discussed before. Most of water molecules are absorbed by the hydrophilic Preyessler HPA, while lesser amounts are absorbed by the hydrophilic regions of NaAlg, thereby leading to easy diffusion of water through the hybrid composite membrane. Sorption study indicated the dominance of solubility selectivity over diffusion selectivity at all the feed water composition. For instance, both sorption and diffusion selectivity values are high at low feed water composition, but with increasing feed water composition, both have decreased. This is expected due to the decrease in membrane separation factor towards water. The increase in flux and decrease in separation factor might be due to decreased interaction between permeants themselves (i.e., water and ethanol) as well as between permeants and membrane at high water compositions. Thus, in the present membranes, PV separation takes place due to the selective adsorption of water molecules onto Preyessler HPA particles, which also is supported by a decrease in contact angle of NaAlg-6 compared to pristine NaAlg-0; this facilitates the easy transport of water through NaAlg-6 membrane by restricting ethanol transport.

Notice that swelling of NaAlg-6 membrane in pure ethanol is smaller than in water, which supports the observed flux data. Increase in flux due to increase in driving force allowing the transport of water as well as its faster desorption on permeate side. This effect is beneficial for water transport, which further justifies the observed increase in separation factor with a recovery of more than 99% of water on the permeate side. The hybrid composite membranes of this study are thus able to dehydrate feed mixtures containing 5–40 wt.% water. Additionally, azeotropic composition of 96 wt.% ethanol was separated by the PV membranes of this study by extracting >99% water on the permeate side.

3.5. Effect of temperature

Temperature plays a considerable role in PV separation. The effect of temperature on PV performance was studied typically for NaAlg-6 membrane for 10 wt.% water containing feed; the resulting flux and separation factor data shown in Fig. 9, suggest that flux

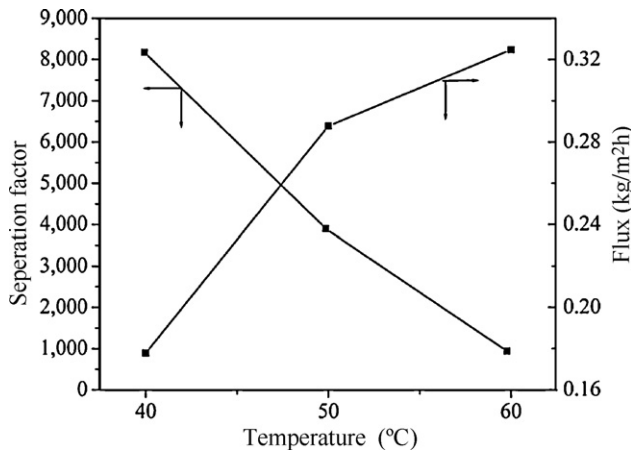


Fig. 9. Effect of temperature on PV performance of NaAlg-6 for 10 wt.% feed water composition.

increased with increasing temperature. In our study, the temperature dependence of permeation and diffusion for water have been calculated using the Arrhenius relationship:

$$X = X_0 \exp\left(\frac{-E_X}{RT}\right) \quad (8)$$

where X represents the diffusion coefficient (D) or permeation flux (J_p), X_0 is a constant representing the pre-exponential factor of D_0 or J_0 , respectively and E_X represents activation energy for permeation or diffusion, depending on the transport process under consideration. As the feed temperature increases, vapor pressure in the feed compartment also increases, but vapor pressure on permeate side is not greatly affected. This would result in increased driving force for mass transfer, consequently resulting in increased permeation flux of the individual penetrant molecule. All these effects tend to support the observed increase in flux and decrease in separation factor with increasing temperature of the feed [38].

From the least squares fit of the linear Arrhenius plots, activation energies for total permeation (E_p), permeation of water (E_{pw}), permeation of ethanol (E_{pe}) and diffusion of water (E_{Dw}) have been determined. The apparent activation energy of water ($E_{pw} = 26.07$ kJ/mol) is much lower than that of ethanol ($E_{pe} = 87.11$ kJ/mol), suggesting that the membrane has higher separation efficiency to water. The activation energy values of water and total permeation ($E_p = 26.31$ kJ/mol) are almost identical, signifying that the coupled-transport of both water and ethanol molecules would be minimal due to higher selective nature of the

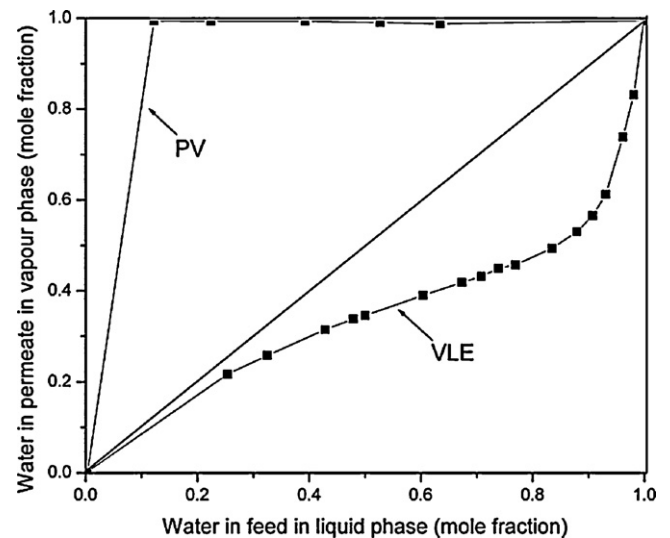


Fig. 10. Comparison of vapor liquid equilibrium curve with PV data for water and ethanol mixtures.

membrane. Further, it is observed that activation energy of permeation of water and that of diffusion of water ($E_{Dw} = 27.85$ kJ/mol) are almost identical to each other, indicating that both permeation and diffusion contribute almost equally to the PV process. Using the above values, we have calculated the heat of sorption:

$$\Delta H_s = E_p - E_D \quad (9)$$

The resulting ΔH_s give information on the transport mechanism of liquids through the membranes. Sorption involves the contributions from Henry's and Langmuir's modes. According to Henry's law, heat of sorption, ΔH_s is positive, thereby leading to absorption of solvent species into that site within the membrane, giving an endothermic contribution to the sorption process. On the other hand, Langmuir's sorption requires the pre-existence of a site in which sorption occurs by hole filling mechanism, giving an exothermic contribution. In the present study, ΔH_s value (-1.78 kJ/mol) is negative, suggesting that Langmuir's sorption is predominant giving an exothermic contribution.

3.6. Comparison of PV results with vapor–liquid equilibrium (VLE) data

Permeate concentration obtained in PV is compared in Fig. 10 with the vapor–liquid equilibrium (VLE) curve obtained from dis-

Table 3

Comparisons of flux and separation factor of Preyssler heteropolyacid-incorporated membranes with literature data at 30 °C.

Membrane type	F_w (wt.%)	β_{ij}	J (kg/m ² h 10 μm)	Ref.
Two-ply composite CS/NaAlg	5.0	1110	0.07	[11]
CS/HEC	10.0	10,491	0.11	[40]
CS/NaAlg	13.5	436	0.22	[41]
P- NaAlg	5.2	2182	0.24	[15]
CS	10.0	8000	0.26	[42]
NaAlg	10.0	120	0.29	[43]
PVA/PVS	6.2	700	0.50	[44]
CS-TEOS (6)	2.0	1380	1.36 ^a	[45]
CS-TEOS (6)	10.0	459	1.4 ^a	[45]
CS-TEOS (6)	10.0	1150	0.24 ^b	[45]
NaAlg-6	4.0 ^c	59,976	0.17	Present work
NaAlg-6	10.0	14,991	0.57	Present work

CS/NaAlg—chitosan/sodium alginate; CS/HEC—chitosan/hydroxyethylcellulose; P-NaAlg—phosphorylated sodium alginate; NaAlg—sodium alginate; PVA/PVS—poly(vinyl alcohol)/poly(styrene sulphuric acid); CS-TEOS—chitosan-tetraethoxysilane.

^c Azeotropic composition.

^a Studied at 80 °C.

^b Studied at 60 °C.

tillation [39]. It is difficult to separate the mixture at its azeotropic composition using the conventional distillation without using an entrainer, such as benzene, a deadly carcinogen. On the other hand, PV is a better alternative option to break the ethanol–water azeotropic composition. In PV, the membrane acts as a third phase in place of benzene as in distillation and selectively allows water molecules to pass through due to its preferential affinity, thus overcoming the azeotropic barrier. Notice that membrane separation factor to water is indeed very high, since permeate is primarily composed of water over the entire composition range of the feed mixture.

3.7. Comparison of present work with literature

A comparison of the present results with the reported data is made in Table 3. The present HPA-incorporated membranes are found to be better than pure NaAlg membranes as well as compared to the literature data for dehydration of ethanol. For instance, the highest separation factor of 59,976 is observed for NaAlg-6 with a flux of 0.172 kg/m² h 10 μm, which is higher than CS/HEC membranes [40] for which separation factor of 10,491 with a flux of 0.11 kg/m² h 10 μm are observed. The lowest value of separation factor of 120 for pure NaAlg with a somewhat higher flux of 0.29 kg/m² h 10 μm distinctly indicates the water-selective nature of the hybrid composite membranes compared to pure NaAlg membrane. Thus, due to the addition of HPA into NaAlg, a drastic increase in membrane separation factor to water occurs, suggesting that the composite hybrid membranes of this study are more efficient for PV dehydration of ethanol than pure NaAlg membrane as well as other membranes developed in the literature. Moreover, the present membranes are mechanically sturdy.

4. Conclusions

Preyssler type HPA was prepared, characterized and used as filler into NaAlg to fabricate composite hybrid membranes with 6, 8 and 10 wt.% loadings. The membranes thus obtained were used in PV separation of water–ethanol mixtures. It is demonstrated that by incorporating Preyssler type HPA particles into NaAlg, the hydrophilicity of NaAlg membrane would enhance due to a discrete structure of HPAs comprising the heteropolyanions and the mobile solvated protons. The membrane flux increased with increasing HPA content, but separation factor decreased due to excess water intake by the membranes. Similarly, PSI of the composite hybrid membranes decreased with increasing filler content of the membranes. Of all the membranes studied, NaAlg-6 showed a good performance in dehydrating ethanol. All the membranes are mechanically stable during the PV runs.

Sorption data revealed that sorption selectivity is higher than diffusion selectivity and hence, sorption seems to play a major role in PV separation of water–ethanol mixture, whereas diffusion seems to play a minor role. Flory–Huggins interaction parameters, χ_{1p} and χ_{2p} revealed that the composite hybrid membranes have a greater affinity to water than ethanol. With increasing feed water composition, the membrane performance was affected markedly probably due to swelling of the polymer, resulting in a rise of flux with a reduction in separation factor. However, even under these conditions, the membranes retained their integrity. The azeotropic composition of water–ethanol mixture (i.e., 4% of water) was separated using the water-selective PV membranes of this study. The composite hybrid membranes have shown significantly lower activation energies for water than ethanol, exhibiting the negative heat of sorption, which suggests that the composite hybrid membranes have good separation ability. Sorption is dominated by Langmuir's mode of sorption due to exothermic contribution to the overall sorption process.

Acknowledgements

G.S.G. and V.T.M. thank the Department of Science and Technology, New Delhi, India (no. SR/S1/PC-31/2006) for a financial support and Department of Physics, Shivaji University for providing contact angle and SEM facilities. T.M.A. thanks the CSIR, New Delhi, India for awarding CSIR Emeritus Scientist [21(0760)/09/EMR-II].

References

- [1] T.M. Aminabhavi, R.S. Khinnavar, S.B. Harogoppad, U.S. Aithal, Q.T. Nguyen, K.C. Hansen, Pervaporation separation of organic–aqueous and organic–organic binary mixtures, *J. Macromol. Sci. Rev. Macromol. Chem. Phys. C* 34 (1994) 139–204.
- [2] S.D. Bhat, T.M. Aminabhavi, Pervaporation separation using sodium alginate and its modified membranes—a review, *Sep. Purif. Rev.* 36 (2007) 203–229.
- [3] I. Blume, J.G. Wijmans, R.W. Baker, The separation of dissolved organics from water by pervaporation, *J. Membr. Sci.* 49 (1990) 253–286.
- [4] P. Shao, R.Y.M. Huang, Polymeric membrane pervaporation, *J. Membr. Sci.* 287 (2007) 162–179.
- [5] S.D. Bhat, N.N. Mallikarjuna, T.M. Aminabhavi, Microporous aluminophosphate (AlPO₄-5) molecular sieve-loaded novel sodium alginate composite membranes for pervaporation dehydration of aqueous–organic mixtures near their azeotropic compositions, *J. Membr. Sci.* 282 (2006) 473–483.
- [6] S.D. Bhat, T.M. Aminabhavi, Zeolite K-LTL-loaded sodium alginate mixed matrix membranes for pervaporation dehydration of aqueous–organic mixtures, *J. Membr. Sci.* 306 (2007) 173–185.
- [7] S.D. Bhat, T.M. Aminabhavi, Novel sodium alginate–Na⁺MMT hybrid composite membranes for pervaporation dehydration of isopropanol, 1,4-dioxane and tetrahydrofuran, *Sep. Purif. Technol.* 51 (2006) 85–94.
- [8] S.D. Bhat, T.M. Aminabhavi, Novel sodium alginate composite membranes incorporated with SBA-15 molecular sieves for the pervaporation dehydration of aqueous mixtures of isopropanol and 1,4-dioxane at 30 °C, *Micropor. Mesopor. Mater.* 91 (2006) 206–214.
- [9] S.D. Bhat, B.V.K. Naidu, G.V. Shanbhag, S.B. Halligudi, M. Sairam, T.M. Aminabhavi, Mesoporous molecular sieve (MCM-41)-filled sodium alginate hybrid nanocomposite membranes for pervaporation separation of water–isopropanol mixtures, *Sep. Purif. Technol.* 49 (2006) 56–63.
- [10] C.K. Yeom, K.H. Lee, Characterization of permeation behaviors of ethanol–water mixtures through sodium alginate membrane with crosslinking gradient during pervaporation separation, *J. Appl. Polym. Sci.* 69 (1998) 1607–1619.
- [11] G.Y. Moon, R. Pal, R.Y.M. Huang, Novel two-ply composite membranes of chitosan and sodium alginate for the pervaporation dehydration of isopropanol and ethanol, *J. Membr. Sci.* 156 (1999) 17–27.
- [12] M.D. Kurkuri, U.S. Toti, T.M. Aminabhavi, Syntheses and characterization of blend membranes of sodium alginate and poly(vinyl alcohol) for the pervaporation separation of water + isopropanol mixtures, *J. Appl. Polym. Sci.* 86 (2002) 3642–3651.
- [13] U.S. Toti, K.S. Soppimath, T.M. Aminabhavi, Sorption, diffusion, and pervaporation separation of water–acetic acid mixtures through the blend membranes of sodium alginate and guar gum-grafted-polyacrylamide, *J. Appl. Polym. Sci.* 83 (2002) 259–272.
- [14] U.S. Toti, T.M. Aminabhavi, Pervaporation separation of water–isopropyl alcohol mixtures with blend membranes of sodium alginate and poly(acrylamide)-grafted guar gum, *J. Appl. Polym. Sci.* 85 (2002) 2014–2024.
- [15] S. Kalyani, B. Smitha, S. Sridhar, A. Krishnaiah, Pervaporation separation of ethanol–water mixtures through sodium alginate membranes, *Desalination* 229 (2008) 68–81.
- [16] S.B. Teli, G.S. Gokavi, M. Sairam, T.M. Aminabhavi, Highly water selective silicotungstic acid (H₄SiW₁₂O₄₀) incorporated novel sodium alginate hybrid composite membranes for pervaporation dehydration of acetic acid, *Sep. Purif. Technol.* 54 (2007) 178–186.
- [17] F.B. Peng, C.L. Hu, Z.Y. Jiang, Novel ploy(vinyl alcohol)/carbon nanotube hybrid membranes for pervaporation separation of benzene/cyclohexane mixtures, *J. Membr. Sci.* 297 (2007) 236–242.
- [18] T.C. Merkel, B.D. Freeman, R.J. Spontak, Z. He, I. Pinnau, P. Meakin, A.J. Hill, Sorption, transport, and structural evidence for enhanced free volume in poly(4-methyl-2-pentyne)/fumed silica nanocomposite membranes, *Chem. Mater.* 15 (2003) 109–123.
- [19] F.B. Peng, Z.Y. Jiang, C.L. Hu, Removing benzene from aqueous solution using CMS-filled PDMS pervaporation membranes, *Sep. Purif. Technol.* 48 (2006) 229–234.
- [20] S. Shanmugam, B. Viswanathan, T.K. Varadarajan, Synthesis and characterization of silicotungstic acid based organic–inorganic nanocomposite membrane, *J. Membr. Sci.* 275 (2006) 105–109.
- [21] P. Staiti, Proton conductive membranes based on silicotungstic acid/silica and polybenzimidazole, *Mater. Lett.* 47 (2001) 241–246.
- [22] M. Helen, B. Viswanathan, S.S. Murthy, Synthesis and characterization of composite membranes based on α-zirconium phosphate and silicotungstic acid, *J. Membr. Sci.* 292 (2007) 98–105.
- [23] S.B. Teli, G.S. Gokavi, M. Sairam, T.M. Aminabhavi, Mixed matrix membranes of poly(vinyl alcohol) loaded with phosphomolybdic heteropolyacid for the pervaporation separation of water–isopropanol mixtures, *Colloid Surf. A* 301 (2007) 55–62.

- [24] P. Staiti, S. Freni, S. Hocevar, Synthesis and characterization of protonconducting materials containing dodecatungstophosphoric and dodecatungstosilic acid supported on silica, *J. Power Sources* 79 (1999) 250–255.
- [25] I.V. Kozhevnikov, Catalysis by heteropolyacids and multicomponent polyoxometalates in liquid-phase reactions, *Chem. Rev.* 98 (1998) 171–198.
- [26] M.H. Alizadeh, T. Keramani, R. Tayebee, A method for the acetylation of alcohols catalyzed by heteropolyoxometalates, *Monatshefte für Chemie* 138 (2007) 165–170.
- [27] T.M. Aminabhavi, H.G. Naik, Synthesis of graft copolymeric membranes of poly(vinyl alcohol) and polyacrylamide for the pervaporation separation of water/acetic acid mixtures, *J. Appl. Polym. Sci.* 83 (2002) 244–258.
- [28] R.Y.M. Huang, C.K. Yeom, Pervaporation separation of aqueous mixtures using crosslinked poly(vinyl alcohol) (PVA) II. Permeation of ethanol-water mixtures, *J. Membr. Sci.* 51 (1990) 273–292.
- [29] S. Wu, W. Zhang, J. Wang, X. Ren, Preyssler-structured tungstophosphoric acid catalyst on functionalized silica for esterification of n-butanol with acetic acid, *Catal. Lett.* 123 (2008) 276–281.
- [30] J.H. Chen, Q.L. Liu, A.M. Zhu, Q.G. Zhang, J. Fang, Pervaporation separation of MeOH/DMC mixtures using STA/CS hybrid membranes, *J. Membr. Sci.* 315 (2008) 74–81.
- [31] N.R. Singha, T.K. Parya, S.K. Ray, Dehydration of 1,4-dioxane by pervaporation using filled and crosslinked polyvinyl alcohol membrane, *J. Membr. Sci.* 340 (2009) 35–44.
- [32] M.H.V. Mulder, C.A. Smolders, On the mechanism of separation of ethanol/water mixtures by pervaporation I. Calculations of concentration profiles, *J. Membr. Sci.* 17 (1984) 289–307.
- [33] J.P.G. Villaluenga, M. Khayet, P. Godino, B. Seoane, J.I. Mengual, Pervaporation of toluene/alcohol mixtures through a coextruded linear low-density polyethylene membrane, *Ind. Eng. Chem. Res.* 42 (2003) 386–391.
- [34] P.J. Flory, *Principles of Polymer Chemistry*, Cornell University Press, Ithaca, NY, 1953.
- [35] D.W. van Krevelen, Chemical structure and properties of coal XXVII-coal construction and solvent extraction, *Fuel* 44 (1965) 229–242.
- [36] J. Gmehling, U. Onken, Vapor–Liquid Equilibrium Data Collection (Aqueous–Organic systems), Schon and Wetzl GmbH, Frankfurt/main, Germany, 2001.
- [37] Q.G. Zhang, Q.L. Liu, Z.Y. Jiang, L.Y. Ye, X.H. Zhang, Effects of annealing on the physico-chemical structure and permeation performance of novel hybrid membranes of poly(vinyl alcohol)/c-aminopropyl-triethoxysilane, *Micropor. Mesopor. Mater.* 110 (2008) 379–391.
- [38] T.M. Aminabhavi, M.B. Patil, S.D. Bhat, A.B. Halgeri, R.P. Vijayalakshmi, P. Kumar, Activated charcoal-loaded composite membranes of sodium alginate in pervaporation separation of water-organic azeotropes, *J. Appl. Polym. Sci.* 113 (2009) 966–975.
- [39] R. Bahrens, Eckermann (Eds.), Vapor–liquid Equilibrium Data Collection, Part 6C, vol. 1, DECHEMA, 1983.
- [40] A. Chanchai, R. Jiratananon, D. Uttapap, G.Y. Moon, A. Anderson, R.Y.M. Huang, Pervaporation with chitosan/hydroxyethylcellulose (CS/HEC) blended membranes, *J. Membr. Sci.* 166 (2000) 271–280.
- [41] P. Kanti, K. Srigowri, J. Madhuri, B. Smitha, S. Sridhar, Dehydration of ethanol through blend membranes of chitosan and sodium alginate by pervaporation, *Sep. Purif. Technol.* 40 (2004) 259–266.
- [42] X.P. Wang, Z.Q. Shen, Zhang, Y.F. Zhang, A novel composite chitosan membrane for the separation of alcohol-water mixtures, *J. Membr. Sci.* 119 (1996) 191–198.
- [43] C.K. Yeom, J.G. Jegal, K.H. Lee, Characterization of relaxation phenomena and permeation behaviors in sodium alginate membrane during pervaporation separation of ethanol-water mixture, *J. Appl. Polym. Sci.* 62 (1996) 1561–1576.
- [44] A. Toutianoush, L. Krasemann, B. Tiede, Polyelectrolyte multilayer membranes for pervaporation separation of alcohol/water mixtures, *Colloids Surf. A* 198 (2002) 881–889.
- [45] J. Ma, M. Jhang, L. Lu, X. Yin, J. Chen, Z. Jiang, Intensifying esterification reaction between lactic acid and ethanol by pervaporation dehydration using chitosan-TEOS hybrid membranes, *Chem. Eng. J.* 155 (2009) 800–809.